Effect of Li Addition on the Microstructure of As-Cast Al-Zn-Mg-Cu-Sc Alloys

DOI: 10.23977/jmpd.2025.090115 ISSN 2516-0923 Vol. 9 Num. 1

Yong Wang, Tiewu Wang, Xiaoming Cui, Fei Liu, Xiaohu Hou, Xueping Zhao, Pucun Bai*

School of Materials Science and Engineering, Inner Mongolia University of Technology, Hohhot, 010051, China
*Corresponding author

Keywords: Al-Zn-Mg-Cu-Sc Alloy, As-Cast, Microstructure

Abstract: This study investigates Al-Zn-Mg-Cu-Sc alloys by introducing varying amounts of Li to achieve synergistic regulation of the alloy microstructure and morphology. Optical microscopy (OM), scanning electron microscopy (SEM), and energy-dispersive spectroscopy (EDS) were employed to analyze the alloys, focusing on the microstructural evolution and variations under different Li additions. The results indicate that the incorporation of Li leads to microstructural refinement, accompanied by the formation of equiaxed grains. Compared with the Li-free alloy, the alloy containing 1.5wt% Li exhibited a 47% reduction in grain size. SEM and EDS analyses further revealed that Al is mainly distributed within the grains, Mg and Zn are dispersed throughout the alloy matrix, while Cu and Sc are enriched at the grain boundaries.

1. Introduction

Al-Zn-Mg-Cu alloys possess a series of advantageous properties, including low density, high strength, good workability, and excellent weldability. The addition of Sc leads to the formation of fine Al₃Sc secondary phases, which can act as heterogeneous nucleation sites, significantly increasing the nucleation rate of aluminum alloys and thereby refining the grain size [1-6].

Microalloying is an effective approach to enhance the performance of Al-Cu-Mg alloys. As a key lightweighting element, lithium (Li) can reduce the alloy's density by approximately 3% and increase the elastic modulus by 6% for every 1 wt% added to aluminum alloys. The addition of Li not only significantly lowers the density but also improves strength through the formation of nano-sized strengthening phases such as $\delta'(Al_3Li)$ and $T_1(Al_2CuLi)$. Moreover, Li effectively promotes the nucleation of GPB zones, delays the nucleation and coarsening of the S phase, thereby significantly enhancing the yield strength of the alloy. Scandium (Sc) also exhibits excellent microalloying effects in Al-Cu-Mg alloys. Trace additions of Sc can lead to the formation of Al $_3$ Sc precipitates, which effectively refine the microstructure and markedly enhance mechanical properties. Li and Sc can couple with Al to form L1 $_2$ -structured phases such as Al $_3$ Sc and Al $_3$ Li, as well as non-equilibrium nano-scale core—shell particles. These unique structures can effectively suppress recrystallization, inhibit grain coarsening, and significantly improve overall alloy performance [7-14].

In aluminum alloys, each 1 wt% increase in Li reduces the alloy density by approximately 3%

and increases the elastic modulus by about 6%. Li can dissolve into the α -Al matrix, resulting in solid-solution strengthening. More importantly, Li promotes the formation of Al₃Li (δ' phase), which is metastable and finely dispersed, thereby significantly enhancing the yield strength and hardness of the alloy. When both Li and Sc are present, Al₃(Sc,Li) composite phases may form, exhibiting improved thermal stability and dispersion-strengthening effects, which contribute to maintaining long-term strength during service.

2. Experiment

2.1 Material preparation

Since Li is highly reactive, it was introduced into the alloy in the form of an Al-Li master alloy to prepare Al-Zn-Mg-Cu-Sc-X%Li alloys (X=0,0.5,1,1.5). The alloy melting was carried out in a ZG-0.03 vacuum induction furnace. The preparation procedure was as follows: prior to melting, the surface impurities of the crucible were thoroughly removed, and the graphite crucible was preheated to 200–300 °C. The alloy raw materials were then charged into the crucible and heated to 750 °C. After complete melting, Al-Li master alloys with different Li contents were introduced into the melt by pressing under a bell jar, followed by stirring with a graphite rod for 20 s to ensure uniform dissolution. Subsequently, refining agents were added, and argon gas was introduced for degassing and refining. The melt temperature was then reduced to approximately 720 °C and held for 10 min, after which it was slowly poured into a preheated metallic mold at 200 °C. After furnace cooling for 30 min, the melt was solidified, and aluminum alloy specimens with different Li mass fractions were obtained.

2.2 Experimental Procedures

The experimental alloys were sectioned into cubic specimens with dimensions of 10 mm ³ and sequentially ground with silicon carbide papers of progressively finer grit sizes to smooth the sample surfaces. The grinding process began with 240# paper and continued up to 2000#. After each change of paper, the specimen was rotated by 90 ° to ensure uniform grinding. When the scratches from the previous grit were completely removed, the next grinding step was initiated.

Following grinding, the specimens were mechanically polished using a P-1 polishing machine. Coarse polishing was performed with 1.5# metallographic polishing paste until most scratches on the surface disappeared, followed by fine polishing with 0.5# metallographic polishing paste until a mirror-like finish was achieved. Metallographic images were then observed and captured using a Zeiss Axio Imager A1m optical microscope manufactured in Germany.

Surface morphology and chemical composition of the specimens were further analyzed using a QUANTA FEG650 scanning electron microscope (SEM) equipped with an Oxford X-max50 energy-dispersive spectrometer (EDS).

3. Results and discussions

3.1 Effect of Li on the as-cast microstructure of the experimental Alloys

Figure 1 shows the optical micrographs (OM) of Al-Zn-Mg-Cu-Sc alloys with different Li additions in the as-cast state. As observed in Figure 1(1), the Al-Zn-Mg-Cu-Sc alloy is mainly composed of primary α -Al together with a low-melting-point Mg(Zn,Cu)₂ eutectic phase distributed along the grain boundaries and interdendritic regions. In the Li-free alloy, the primary α -Al exhibits a coarse dendritic morphology with irregular shapes. The Mg(Zn,Cu)₂ eutectic phase appears as

coarse needle-like or plate-like structures, semi-continuously distributed along the α -Al dendritic boundaries, and occupying a relatively large area fraction.

By contrast, Figures 1(2)–(4) clearly demonstrate that with the addition of Li, the alloy microstructure becomes refined. The dendrite arm spacing of α -Al decreases, the number of dendrites is reduced, and equiaxed grains appear, resulting in a relatively uniform microstructural distribution. Meanwhile, the Mg(Zn,Cu)₂ eutectic phase becomes finer. In particular, in the alloy containing 1.5 wt% Li, a considerable amount of irregular eutectic structures is observed within the grains.

Since the main role of Li in as-cast Al-Zn-Mg-Cu-Sc alloys is to enhance the precipitation-hardening response during aging, the grain refinement effect of Li addition in the as-cast state is not particularly pronounced.

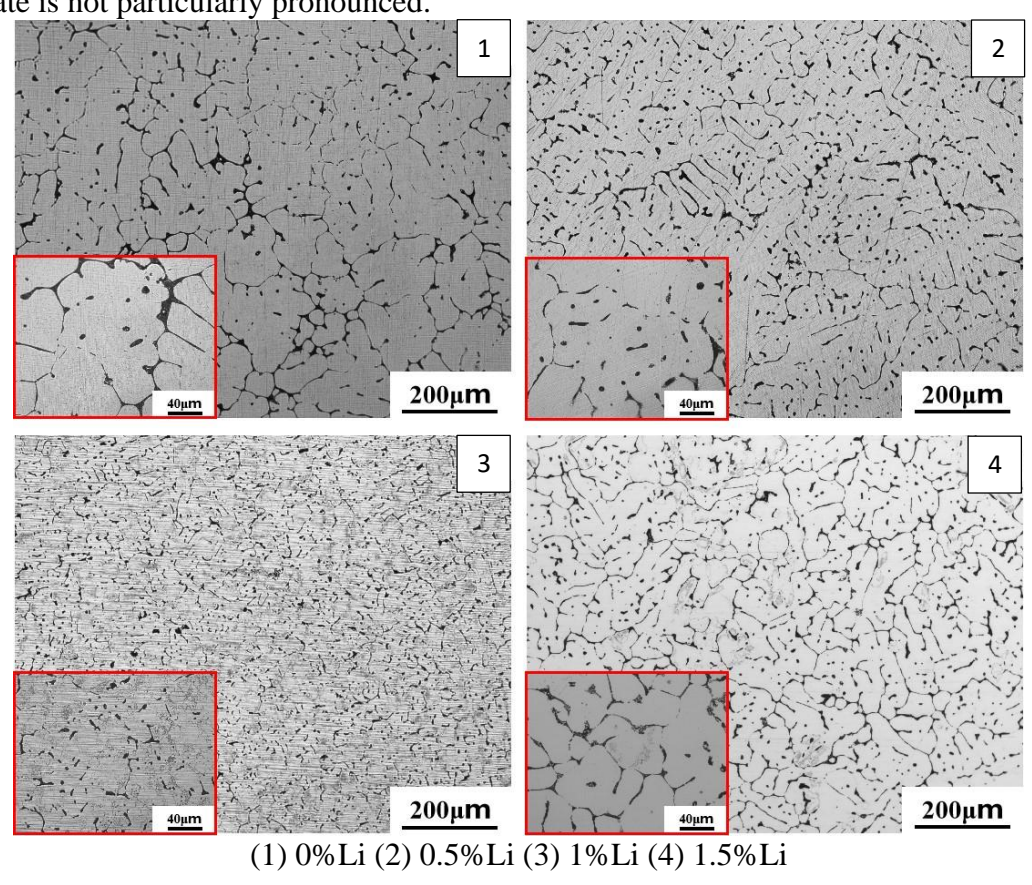


Figure 1 Photos of metallographic structure of experimental alloys with different Li contents

The grain size of α -Al in the experimental alloys with different Li contents was measured using Nano Measurer software, and the results of the four alloys were plotted together, as shown in Figure 2. As illustrated in Figure 2, the α -Al grain size distribution in the Li-free alloy is relatively wide, with the smallest grain size of approximately 70 μ m, the largest up to 250 μ m, and an average grain size of 154.12 μ m. With the addition of 0.5 wt% Li, the number of grains in the alloy increases significantly, and the average α -Al grain size decreases to 115.38 μ m. When the Li content reaches 1 wt%, the average α -Al grain size further decreases to 102.72 μ m. At 1.5 wt% Li, the α -Al grains become more uniformly distributed, mainly within the range of 50–120 μ m, with an average grain size of 81.37 μ m.

Overall, as the Li content increases, the average grain size of α -Al exhibits a decreasing trend. Compared with the Li-free alloy, the grain size in the 1.5 wt% Li alloy is reduced by 47%, with the minimum average grain size obtained at 1.5 wt% Li. Based on the microstructural observations and

analysis, it can be concluded that the optimal alloying effect in the as-cast Al-Zn-Mg-Cu-Sc alloy is achieved with the addition of 1.5 wt% Li.

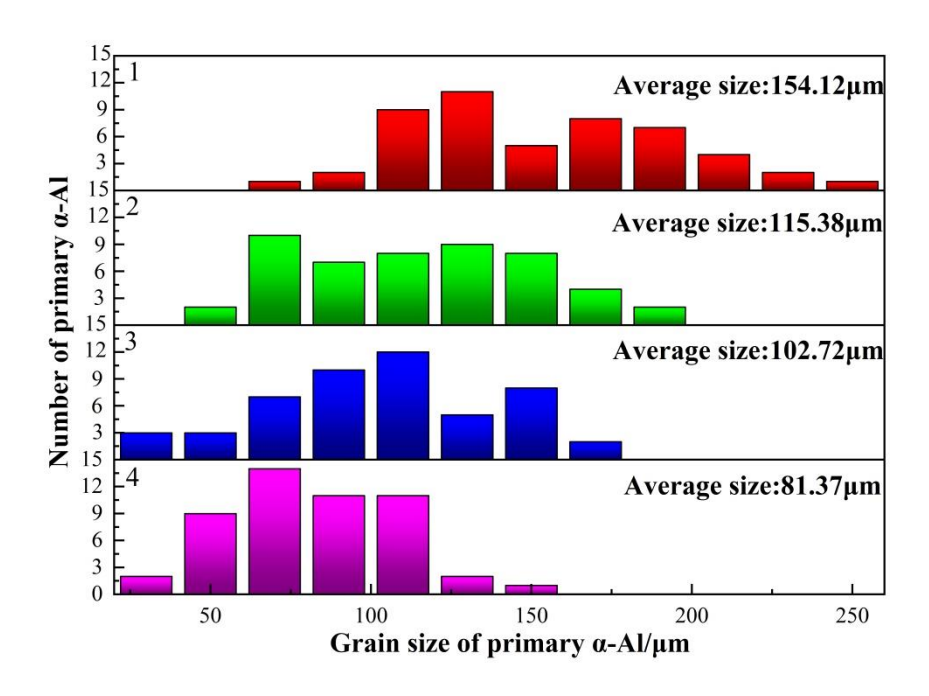


Figure 2 Average grain size distribution of α -Al with different Li contents

3.2 SEM and EDS analysis of the experimental alloys

Figure 3 presents the SEM micrographs and corresponding element mapping images of Al-Zn-Mg-Cu-Sc alloys containing 0 wt% and 1.5 wt% Li in the as-cast state. As shown in the SEM image of Figure 3(1), in the absence of Li, the alloy contains coarse secondary phases, mainly distributed along the grain boundaries in a lamellar and relatively continuous morphology. Within the grains, spherical precipitates of secondary phases and a small number of defects can be observed. In contrast, Figure 3(2) shows that after the addition of 1.5wt% Li, most of the lamellar structures at the grain boundaries disappear, partly transforming into a honeycomb-like morphology, while some grain boundaries exhibit discontinuous refinement. The secondary phases become discontinuous and show signs of refinement, with many fragmenting into block-like structures. The intragranular spherical phases are reduced, accompanied by the formation of small, dispersed short rod-like or blocky phases, as well as irregular eutectic structures with partially continuous morphologies.

The element mapping images further reveal the elemental distribution in the alloys. For the 0 wt% Li alloy (Figure 3(1)), the five principal alloying elements (Al, Cu, Mg, Zn, and Sc) display distinct distribution patterns. Al is mainly distributed within the grains, with little presence at the grain boundaries or in the intragranular secondary phases. Cu is heavily enriched at the grain boundaries, forming a large number of continuously distributed, skeleton-like eutectic phases. Mg is primarily distributed within the grains, with relatively little at the grain boundaries. Zn is more uniformly distributed throughout the alloy, while Sc shows segregation at the grain boundaries as well as a small amount of dispersed distribution within the grains. For the 1.5 wt.% Li alloy (Figure 3(2)), the overall distributions of Al, Cu, Mg, Zn, and Sc remain essentially similar, however, the amount of Cu-rich eutectic phases at the grain boundaries decreases as the eutectic content is reduced. It should be noted that Li distribution does not appear in the mapping results of either alloy, as EDS cannot detect Li.

Given that lithium has an atomic number of 3 with an electronic configuration of 2s^1, and possesses a relatively small atomic radius, Li atoms tend to preferentially occupy lattice vacancies in crystal structures, particularly in common structures such as face-centered cubic (FCC). Based on the SEM and mapping results, it can be inferred that the refinement of grains after Li addition may result from its suppression of the diffusion of other elements. Specifically, Li atoms preferentially occupy lattice vacancies, thereby hindering grain growth. Furthermore, the observed reduction of eutectic phases at grain boundaries may also be attributed to the influence of Li on the diffusion rates of other alloying elements, which in turn inhibits the formation of eutectic structures.

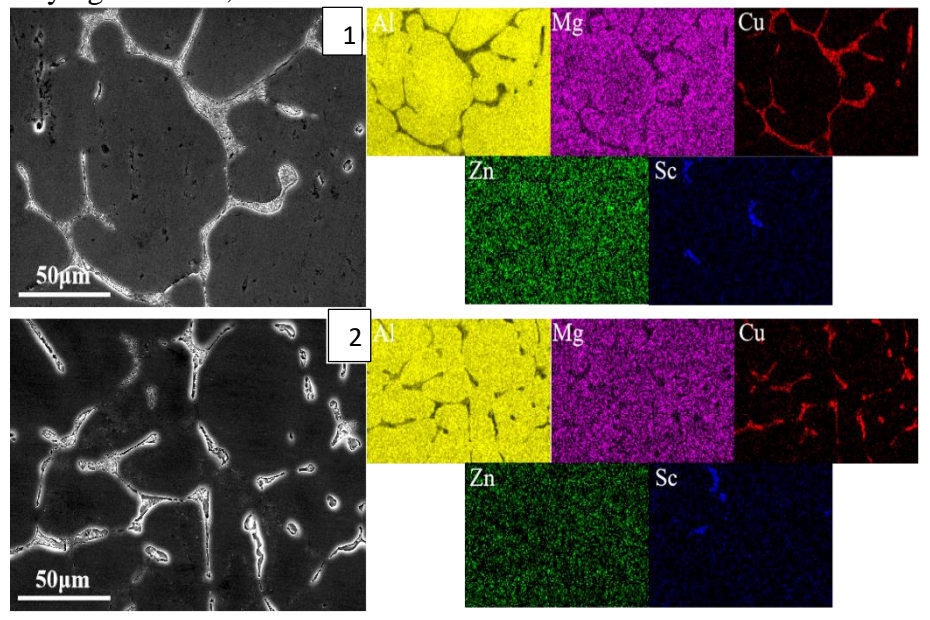


Figure 3 SEM and mapping results of alloys with varying Li content: (1): 0%Li (2): 1.5%Li

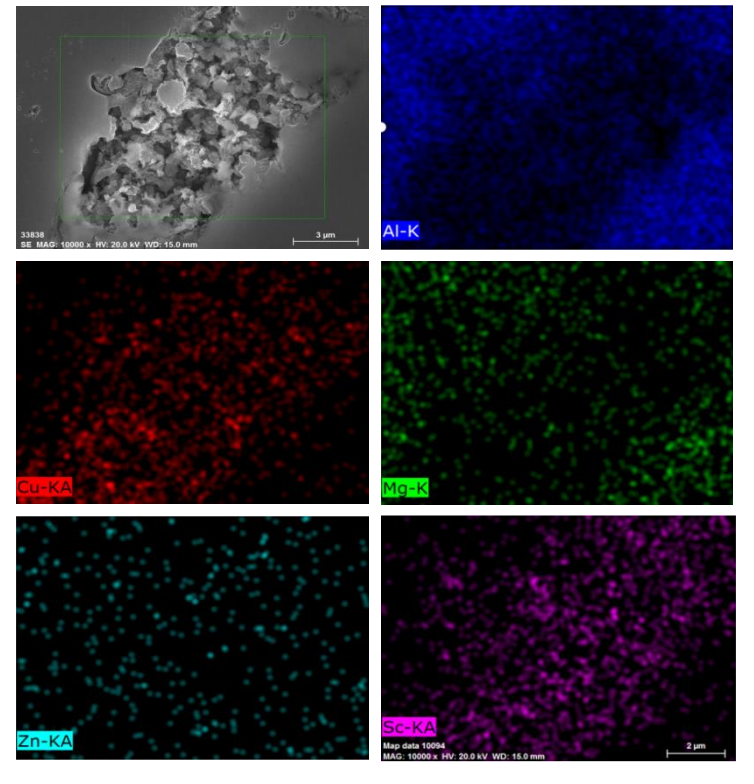


Figure 4 SEM and mapping results at the grain boundaries of the 1.5% Li alloy

To further clarify the segregation of Sc observed at the grain boundaries in Figure 3, higher-magnification images were acquired for detailed analysis. Figure 4 shows the element mapping of the grain boundaries in the alloy containing 1.5 wt.% Li. It can be observed that Al remains primarily distributed within the grains, while Cu and Sc are mainly concentrated at the grain boundaries. Mg is predominantly located within the grains with only a small fraction at the grain boundaries, and Zn is distributed uniformly both within the grains and along the boundaries. In particular, Sc is mainly enriched in the honeycomb-like eutectic phases, suggesting the possible presence of Al₃Sc at these sites.

When Sc is introduced into Al-Zn-Mg-Cu alloys, due to diffusion limitations under normal solidification conditions, Sc tends to segregate at the solid–liquid interface during solidification. This segregation promotes solute redistribution, which increases the constitutional undercooling of the alloy, thereby intensifying the dendritic growth process and resulting in finer dendritic cells. Moreover, the nanoscale Al₃Sc particles formed during solidification act as heterogeneous nucleation sites, further contributing to grain refinement in the alloy.

In summary, for the Al-Zn-Mg-Cu-Sc alloy without Li addition, Al is mainly distributed within the grains, Cu is concentrated at the grain boundaries and in intragranular secondary phases, Mg is primarily distributed inside the grains, and Zn is relatively uniformly distributed throughout the alloy. After the addition of 1.5 wt% Li, Al remains distributed within the grains, while Mg and Zn are dispersed throughout the alloy matrix, and Cu and Sc are enriched at the grain boundaries. The Al₃Sc phase serves as a nucleation agent, thereby contributing to grain refinement.

Energy-dispersive spectroscopy (EDS) was conducted on the SEM images in Figures 3(1) and (2), and the results are summarized in Table 1. From these data, it can be inferred that in the alloy without Li, the lamellar eutectic phases at the grain boundaries and the spherical precipitates inside the grains are both Mg(Zn,Cu)₂ phases. In the alloy containing 1.5 wt% Li, the blocky eutectic phases at the grain boundaries, the spherical precipitates within the grains, and the finely dispersed short rod-like or blocky phases are also identified as Mg(Zn,Cu)₂phases. Due to the small scale of the intragranular short rod-like precipitates, a relatively high Al content appears in the EDS measurements.

							1
Alloy	Position	Zn	Mg	Cu	Sc	Al	Precipitate
0%Li	A	2.15	3.21	0.52	/	94.12	α-Al
	В	8.6	11.29	8.01	/	72.1	$Mg(Zn,Cu)_2$
	С	7.68	15.8	9.8	/	66.72	$Mg(Zn,Cu)_2$
1.5%Li	D	2.1	2.6	0.4	0.24	94.66	α-Al
	Е	7.92	8.83	4.48	/	78.76	$Mg(Zn,Cu)_2$
	F	1.39	2.42	2.56	/	93.63	$Mg(Zn,Cu)_2$
	G	8.55	10.63	4.93	/	75.9	Mg(Zn,Cu) ₂

Table 1 EDS Results of Different Phases in As-Cast 0% Li and 1.5% Li Alloys (at.%)

4. Conclusion

This study investigated the effect of Li on the microstructure of as-cast Al-Zn-Mg-Cu-Sc alloys. The main conclusions are as follows:

- (1) The optimal alloying effect in the as-cast Al-Zn-Mg-Cu-Sc alloy is achieved with the addition of 1.5wt.% Li. Compared with the Li-free alloy, the alloy containing 1.5wt% Li exhibited a 47% reduction in grain size.
- (2) Al is mainly distributed within the grains, Mg and Zn are dispersed throughout the alloy matrix, while Cu and Sc are enriched at the grain boundaries.

Acknowledgments

This work was supported by the Natural Science Foundation of Inner Mongolia Autonomous Region (No. 2024MS05030), the Inner Mongolia Key Research and Results Transformation Project (2023YFHH0045), the Natural Science Foundation of Inner Mongolia Autonomous Region (2023LHMS05015), and the Basic Scientific Research Project for Universities Directly under the Inner Mongolia Autonomous Region (JY20240011).

References

- [1] Huang R, Yang H, Zheng S, et al. The evolution mechanism of the second phase during homogenization of Al-Zn-Mg-Cu aluminum alloy[J]. Materials & Design, 2023, 235: 112395.
- [2] Sharma M M, Amateau M F, Eden T J. Hardening mechanisms of spray formed Al–Zn–Mg–Cu alloys with scandium and other elemental additions[J]. Journal of Alloys and Compounds, 2006, 416(1-2): 135-142.
- [3] Starke Jr E A, Staley J T. Application of modern aluminum alloys to aircraft[J]. Progress in aerospace sciences, 1996, 32(2-3): 131-172.
- [4] J. Zhang, G. Wu, L. Zhang, X. Zhang, C. Shi, X. Tong, Addressing the strength-ductility trade-off in a cast Al-Li-Cu alloy—Synergistic effect of Sc-alloying and optimized artificial ageing scheme, Journal of Materials Science & Technology, 96 (2022) 212-225.
- [5] B. Wang, Q. Zhao, F. Qiu, Q. Jiang, Effect of Mg and Si contents and TiC nanoparticles on the center segregation susceptibility of twin-roll cast Al-Mg-Si alloys, Journal of Materials Research and Technology, 25 (2023) 411-419.
- [6] P. Deng, W. Mo, Z. Ouyang, C. Tang, B. Luo, Z. Bai, Mechanical properties and corrosion behaviors of (Sc, Zr) modified Al-Cu-Mg alloy, Materials Characterization, 196 (2023) 112619.
- [7] L. Chen, K. Liu, R. Su, G. Li, Effect of Sn element on microstructure and mechanical properties of Al-Cu-Mg alloy, Materials Today Communications, 45 (2025) 112383.
- [8] Debin Zhao, Xiaoyi Yuan, Mengyuan Han, Hao Fan, Modulation of the organization and properties of Al-Cu Alloys by alloying elements[J]. Metallurgical Engineering, 2025, 12: 58.
- [9] Li Q, Wu A, Li Y, et al. Influence of temperature cycles on the microstructures and mechanical properties of the partially melted zone in the fusion welded joints of 2219 aluminum alloy[J]. Materials Science and Engineering: A, 2015, 623: 38-48.
- [10] Abdelaziz M H, Elgallad E M, Doty H W, et al. Strengthening precipitates and mechanical performance of Al–Si–Cu–Mg cast alloys containing transition elements[J]. Materials Science and Engineering: A, 2021, 820: 141497.
- [11] Yang H, Liu Y, Li Y, et al. Influence of Cu/Mg ratio and content on heat-resistance of Al–Cu–Mg alloys[J]. Journal of Materials Research and Technology, 2024, 29: 1040-1051.
- [12] Gu J, Ding J, Williams S W, et al. The effect of inter-layer cold working and post-deposition heat treatment on porosity in additively manufactured aluminum alloys[J]. Journal of materials processing technology, 2016, 230: 26-34.
- [13] Liang S S, Wei W, Wen S P, et al. Enhanced thermal-stability of AlCuMg alloy by multiple microalloying segregation of Mg/Si/Sc solute[J]. Materials Science and Engineering: A, 2022, 831: 142235.
- [14] Rometsch P A, Zhu Y, Wu X, et al. Review of high-strength aluminium alloys for additive manufacturing by laser powder bed fusion[J]. Materials & Design, 2022, 219: 110779.